PHYSICAL REVIEW B VOLUME 15, NUMBER 1 1 JANUARY 1977

Energy bands in ferromagnetic nickel*

C. S. Wang and J. Callaway
Department of Physics and Astronomy, Louisiana State University, Baton Rouge, Louisiana 70803
(Received 9 August 1976)

Energy bands in ferromagnetic nickel are calculated self-consistently using two different potentials: the Kohn-Sham-Gaspar local-exchange approximation and the spin-polarized exchange-correlation potential of von Barth and Hedin. The linear-combination-of-atomic-orbitals method was employed using a basis set of independent Gaussian orbitals. Spin-orbit coupling and other relativistic effects were ignored. Improved techniques for the calculation of the exchange potential and for integrations over the Brillouin zone have been developed and applied. Use of the exchange-correlation potential leads to significant improvement in the magneton number and the exchange splitting. Results are also presented for charge and spin form factors, contact charge densities, and the Fermi surface.

I. INTRODUCTION

In previous publications, we have reported self-consistent calculations of energy bands in ferromagnetic nickel using the linear-combination-of-atomic-orbitals method[1,2] and the Kohn-Sham-Gaspar[3] (KSG) local-exchange approximation. The basis set consisted of atomic wave functions for the $1s$, $2s$, $3s$, $4s$, $2p$, $3p$, and $4p$ states plus five independent d-type Gaussian orbitals. Results obtained were in reasonable agreement with a variety of experimental measurements. In order to determine whether the remaining discrepancies between theory and experiment could be removed by calculations using improved techniques, the self-consistent calculations were repeated with several major changes in the programs. The results largely confirmed previous findings; however, substantially more precise results were obtained for wave functions, particularly of s and p type. We concluded that most of the disagreement between theory and experiment should be attributed to inadequacy of the basic model. We have therefore repeated the self-consistent calculation using the spin-polarized exchange-correlation potential of von Barth and Hedin[4] (vBH), which modifies the KSG exchange potential through inclusion of some correlation effects. Significant improvements are found in the calculated magneton number and in the exchange splitting.

This paper is organized as follows. In Sec. II, we describe several different improvements that have been made in our computational techniques. Our results are presented in Sec. III, where they are compared with experiment. The residual discrepancies between theory and experiment are discussed. The conclusions are stated in Sec. IV.

II. PROCEDURES

The Bloch wave functions are expanded in a set of independent Gaussian orbitals including thirteen s type, ten p type, five d, and one f. This extends our previous work in which atomic wave functions were used for all states except $3d$ and f orbitals were not included. The use of independent orbitals should lead to improved wave functions particularly for s and p states. The Hamiltonian and overlap matrices have dimension 75×75. The exponents of the s, p, and d orbitals were those used by Wachters[5] in a self-consistent calculation for the free nickel atom, except that the s and p orbitals of longest range were deleted. Very-long-range orbitals contribute little to a band calculation and cause severe problems with extensive overlap and approximate linear dependence. The f orbital was chosen to have the exponent 0.8. Spin-orbit coupling is neglected in the present calculation. The changes in the Fermi surface and other properties due to spin-orbit coupling have been considered previously, and do not concern the questions studied here.

The essential features of the computational techniques used in our previous work have been discussed elsewhere.[1,2,6,7] Significant improvements have been made. A detailed account of our current programs will be published in another journal. Here we will give a brief discussion of five major changes. The first concerns the construction of the Fourier coefficients of the starting exchange potential for the iterative process leading to self-consistency. The atomic cell is divided into three regions. The charge density is in the innermost region ($r<1$ a.u.) is spherically symmetric. In the region between 1 a.u. and $r=\frac{1}{2}a$ (a is the lattice constant), the exchange potential is expanded in a series of Kubic harmonics up to the eighth order. The angular part of the Fourier transform is carried out analytically and Filon's rule including 400 points in the range is used to perform the radial integrals. In order to include the contribution from the interstitial region between the inscribed sphere and the cell boundary the irreduci-

ble wedge of the unit cell was partitioned into 1785 cubes and the exchange potential was interpolated linearly inside each cube.

Second, the computation of the changes in the exchange potential in the iterative process leading to the self-consistency has been modified as follows: The change in the exchange potential as the iterations progress is small compared to the initial quantity. Hence it is legitimate to retain only first-order terms in the expansion of the exchange (or exchange correlation potential) in terms of the change in charge density compared to starting density. Let $f(\rho)$ be the relevant function of the charge density, and let f_K denote the coefficients in its Fourier expansion

$$f(\rho) = f(\rho_0) + f'(\rho_0)\delta\rho. \tag{1}$$

Then

$$f_K = f_{0,K} + \sum_{t} f'_{K-K'}\delta\rho_{K'}, \tag{2}$$

in which $f'_{K-K'}$ is a Fourier coefficient of f', and $f_{0,K}$ refers to $f(\rho_0)$. For example, for the KSG exchange potential,

$$V_{x\sigma} = -2e^2[(3/4\pi)\rho_\sigma]^{1/3}, \tag{3}$$

the change in $V_x(K_S)$ is then

$$\delta V_{x\sigma,\vec{k}} = -\frac{2e^2}{3}\left(\frac{3}{4\pi}\right)^{1/3}\sum_{\vec{k}'}(\rho_{0,\sigma}^{-2/3})_{\vec{k}-\vec{k}'}\delta\rho_{\vec{k}'}. \tag{4}$$

A somewhat similar expression is obtained for the vBH potential. The Fourier coefficients of the change in charge density $\delta\rho_{\vec{k}}$ are required for the computation of the changes in the Coulomb potential, and are available in our program. Hence, if we compute the Fourier coefficients of the derivatives of the exchange-correlation potential, it is possible to find the Fourier coefficients of this potential corrected for small changes in the charge density. In $\vec{r}$ space, $\rho_{0\sigma}^{-2/3}$ is smooth near the boundary of the unit cell, and small near the center, therefore we would expect $(\rho_{0\sigma}^{-2/3})_K$ to be significant only for modest values of K. The sum in (4) should converge readily, and our experience shows that this is the case. We retain the lowest 20 Fourier coefficients of the changes in the exchange potential and keep the first 40 $\delta\rho_{\vec{k}'}$ in (4) to calculate these.

Third, we have modified the programs to include an Ewald-type procedure for the calculation of matrix elements of the Coulomb potential in a manner similar to that described by Chaney *et al.*[8] In this procedure, the crystal potential $V_c(\vec{r})$ is separated into two parts,

$$V_c(\vec{r}) = V_l(\vec{r}) + [V_c(\vec{r}) - V_l(\vec{r})],$$

in which the localized potential $V_l(\vec{r})$ has a Coulomb singularity at each nuclear site but vanishes at the boundaries of each unit cell, while the difference $V_c(\vec{r}) - V_l(\vec{r})$ is not singular and is expanded in a Fourier series in the reciprocal lattice. The following form was found to be convenient for $V_l(\vec{r})$

$$V_l(\vec{r}) = -(Ze^2/r)e^{-\beta_1 r^2} + (\alpha/r)(e^{-\beta_1 r^2} - e^{-\beta_2 r^2}). \tag{5}$$

The second term represents a part of the potential of the electron distribution.

Fourth, we have adopted the procedure of Chaney and Dorman for the calculation of the matrix elements of $\cos\vec{K}\cdot\vec{r}$.[9] This greatly simplified the calculation of the matrix elements, especially those involving f orbitals.

Fifth, Brillouin-zone integrals are calculated using a linear analytic method in which the irreducible $\frac{1}{48}$th of the Brillouin zone is divided into tetrahedra.[10,11] The advantage is that the contribution from the occupied portion of a given tetrahedron can be evaluated exactly. This is particularly helpful in the case of nickel where the $L'_{2\downarrow}$ state sometimes oscillates about the Fermi energy in the iterative procedure toward self-consistency.

Comparison of calculations with the Kohn-Sham exchange potential, Eq. (3) with experiment as described in Sec. III indicates that the calculated magnetic moment and exchange splitting are too large. The Kohn-Sham potential evidently overestimates the tendency toward ferromagnetism, and this overestimate should be reduced through the use of a potential which incorporates additional correlation effects. Such a potential has been introduced by von Barth and Hedin.[4] Instead of (3), the exchange potential for electrons of spin σ is

$$V_{xc,\sigma} = A(\rho)(2\rho_\sigma/\rho)^{1/3} + B(\rho), \tag{6}$$

in which $\rho = \rho_\uparrow + \rho_\downarrow$ is the total charge density. Parameterized forms for A and B are given in Ref. 4. In order to reduce storage requirements in the iterative process leading to self-consistency, we expand (6) to first order in the difference between majority and minority spin densities before applying (1).

III. RESULTS AND COMPARISON WITH EXPERIMENTS

The band structure of nickel has been calculated self-consistently for both the KSG and vBH potentials using the procedures described in Refs. 1 and 2 modified as specified above. All calculations were made for the observed lattice constant extrapolated to $T = 0$ °K ($a = 6.644$ a.u.). The criteria of self-consistency was that in the last iteration, no Fourier coefficients of potential (either Coulomb or exchange) should change by more than 4×10^{-5} Ry. The charge density was sampled at 89

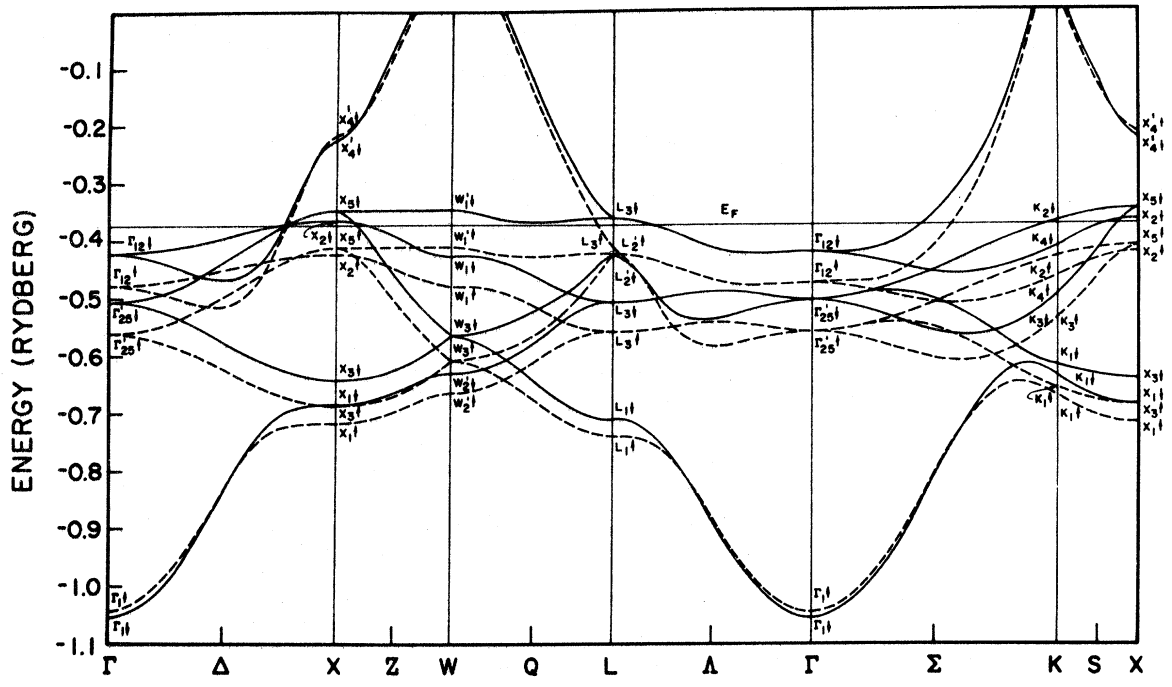

FIG. 1. Energy bands in nickel along several symmetry directions according to the Kohn-Sham potential. Majority spin states are denoted by a dashed line; minority spins by a solid line.

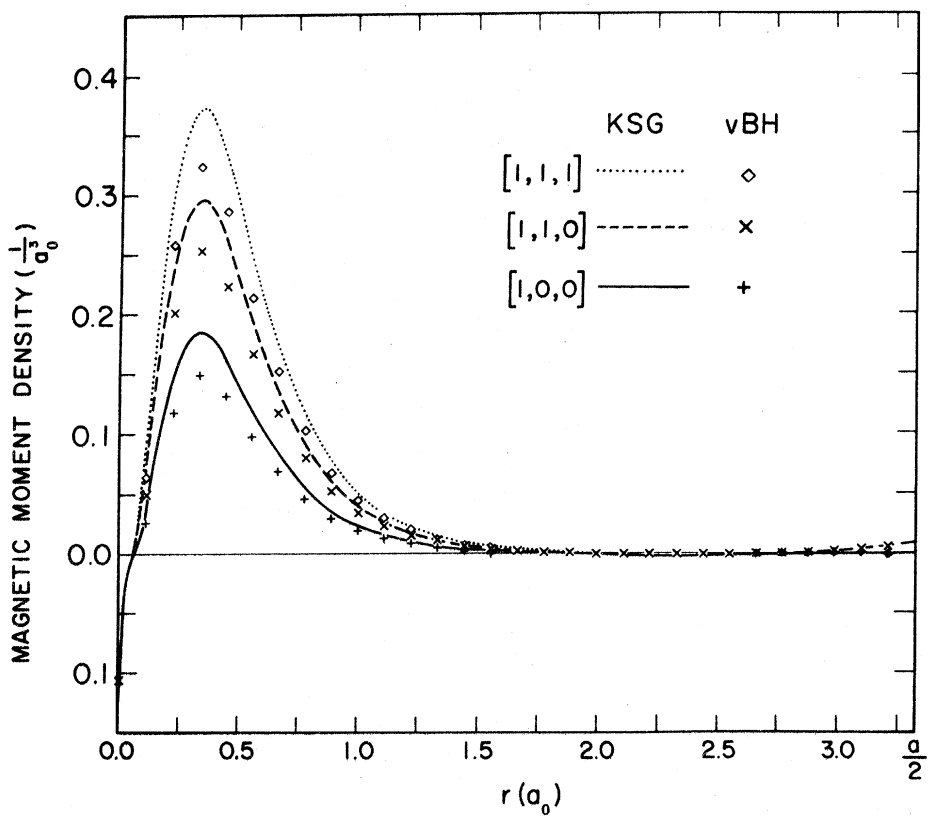

FIG. 2. Calculated magnetic moment densities along three directions according to the KSG potential and the vBH potential. The curves and points are indicated on the figure.

TABLE I. Energies (in rydbergs) determined in the Kohn-Sham potential, Eq. (3), of the lowest six states above the core at symmetry points of the Brillouin zone. The number in parentheses following the energy designates the irreducible representation.

Band	$\Gamma(000)$	$X(100)$	$W(1\frac{1}{2}0)$	$L(\frac{1}{2}\frac{1}{2}\frac{1}{2})$	$K(\frac{3}{4}\frac{3}{4}0)$
			Majority spin		
1	−1.0437(1)	−0.7180(1)	−0.6657(2′)	−0.7409(1)	−0.6715(1)
2	−0.5603(25′)	−0.6869(3)	−0.6099(3)	−0.5605(3)	−0.6587(1)
3	−0.5603(25′)	−0.4238(2)	−0.6099(3)	−0.5605(3)	−0.5389(3)
4	−0.5603(25′)	−0.4123(5)	−0.4818(1)	−0.4246(3)	−0.4655(4)
5	−0.4771(12)	−0.4123(5)	−0.4122(1′)	−0.4246(3)	−0.4314(2)
6	−0.4771(12)	−0.2159(4′)	+0.1772(3)	−0.4167(2′)	+0.0300(3)
			Minority spin		
1	−1.0531(1)	−0.6852(1)	−0.6317(2′)	−0.7121(1)	−0.6361(1)
2	−0.5050(25′)	−0.6413(3)	−0.5669(3)	−0.5083(3)	−0.6174(1)
3	−0.5050(25′)	−0.3651(2)	−0.5669(3)	−0.5083(3)	−0.4955(3)
4	−0.5050(25′)	−0.3478(5)	−0.4285(1)	−0.4273(2′)	−0.4104(4)
5	−0.4213(12)	−0.3478(5)	−0.3477(1′)	−0.3629(3)	−0.3681(2)
6	−0.4213(12)	−0.2245(4′)	+0.1875(3)	−0.3629(3)	+0.0426(3)
			$E_F = -0.3747$		

points in $\frac{1}{48}$th of the Brillouin zone. After completion of the calculation of the self-consistent potentials, energy levels and wave functions were obtained at 505 points in $\frac{1}{48}$th of the Brillouin zone.

Energy levels along certain symmetry lines are shown in Fig. 1 for the KSG potential. In general, the relative position of the energy levels agrees quite closely with that reported in Ref. 1 (difference of 0.01 Ry or less, except for X_4'). The most interesting change is that the exchange splitting of certain of the s and p states is now negative (Γ_1, L_2', X_4'). This results from a predominance of minority spin density (Fig. 2) both close to the nuclei and in the outer portion of the atomic cell.

The inclusion of the correlation potential lowers the energy levels typically in the range 0.14–0.16 Ry, and reduces the exchange splitting of the d states by roughly 0.015 Ry. Detailed comparison of Kohn-Sham and vBH energy levels can be found in Tables I and II where energies of selected states at the symmetric points Γ, X, W, L, and K (and the Fermi energy) are tabulated. It will be observed that the exchange splitting of states near the top of the d band (X_5, W_1') is 0.0645 (0.88 eV) with the KSG potential but is reduced to 0.0463 Ry (0.63 eV) with the vBH potential. There is a corresponding

TABLE II. Energies (in rydbergs) determined in the vBH potential, Eq. (5), of the lowest six states above the core at symmetry points of the Brillouin zone. The number in parentheses following the energy designates the irreducible representation.

Band	$\Gamma(000)$	$X(100)$	$W(1\frac{1}{2}0)$	$L(\frac{1}{2}\frac{1}{2}\frac{1}{2})$	$K(\frac{3}{4}\frac{3}{4}0)$
			Majority spin		
1	−1.1890(1)	−0.8632(1)	−0.8108(2′)	−0.8855(1)	−0.8166(1)
2	−0.7043(25′)	−0.8311(3)	−0.7541(3)	−0.7051(3)	−0.8031(1)
3	−0.7043(25′)	−0.5689(2)	−0.7541(3)	−0.7051(3)	−0.6831(3)
4	−0.7043(25′)	−0.5561(5)	−0.6269(1)	−0.5689(3)	−0.6106(4)
5	−0.6222(12)	−0.5561(5)	−0.5561(1′)	−0.5689(3)	−0.5753(2)
6	−0.6222(12)	−0.3616(4′)	0.0320(3)	−0.5620(2′)	−0.1151(3)
			Minority spin		
1	−1.1923(1)	−0.8382(1)	−0.7849(2′)	−0.8630(1)	−0.7896(1)
2	−0.6643(25′)	−0.7976(3)	−0.7222(3)	−0.6673(3)	−0.7725(1)
3	−0.6643(25′)	−0.5264(2)	−0.7222(3)	−0.6673(3)	−0.6507(3)
4	−0.6643(25′)	−0.5098(5)	−0.5881(1)	−0.5659(2′)	−0.5706(4)
5	−0.5818(12)	−0.5098(5)	−0.5098(1′)	−0.5245(3)	−0.5298(2)
6	−0.5818(12)	−0.3640(4′)	0.0420(3)	−0.5245(3)	−0.1037(3)
			$E_F = -0.5342$		

TABLE III. Contact charge densities. "Band" refers to the sum of contribution from the occupied states above the core (including s-d hybridization). All quantities are in atomic units (a_0^{-3}). The net spin density is equivalent to an effective hyperfine field of −69.7 kG for the KSG potential and −57.6 kG for the vBH potential.

j	$\lvert\psi_{j\uparrow}(0)\rvert^2$	$\lvert\psi_{j\downarrow}(0)\rvert^2$	$\lvert\psi_{j\uparrow}(0)\rvert^2+\lvert\psi_{j\downarrow}(0)\rvert^2$	$\lvert\psi_{j\uparrow}(0)\rvert^2-\lvert\psi_{j\downarrow}(0)\rvert^2$
Kohn-Sham 1s	6491.881	6491.918	12 983.799	−0.037
Kohn-Sham 2s	602.540	602.782	1205.322	−0.242
Kohn-Sham 3s	88.312	88.091	176.403	0.221
Kohn-Sham band	2.986	3.061	6.047	−0.075
Kohn-Sham total	7185.719	7185.852	14 371.571	−0.133
vBH 1s	6463.165	6463.189	12 926.354	−0.024
vBH 2s	601.109	601.321	1202.430	−0.212
vBH 3s	88.057	87.878	175.935	0.179
vBH band	2.948	3.002	5.950	−0.053
vBH total	7155.280	7155.390	14 310.670	−0.110

shift of peak positions in the density of states as will be shown subsequently. A precise experimental value for a typical exchange splitting is not known, however, our previous analysis of the optical conductivity suggests 0.5 eV for this quantity.[2] Better agreement with the experimentally measured magneton number[12] (0.56) is also found with vBH potential (0.58) than the KSG potential (0.65). The difference between the latter value and our previous result[2] (0.62) is principally due to the use of

TABLE IV. Spin-density form factor.

Wave vector $a\vec{K}/2\pi$	Present KSG	Present vBH	Wakoh and Yamashita (Ref. 14)	Expt. (Ref. 15)
(0, 0, 0)	1.000	1.000		
(1, 1, 1)	0.790	0.762	0.766	0.793 ± 0.009
(2, 0, 0)	0.697	0.669	0.665	0.703 ± 0.008
(2, 2, 0)	0.440	0.423	0.419	0.447 ± 0.005
(3, 1, 1)	0.309	0.297	0.296	0.321 ± 0.005
(2, 2, 2)	0.295	0.285	0.287	0.311 ± 0.004
(4, 0, 0)	0.160	0.152	0.154	0.157 ± 0.003
(3, 3, 1)	0.153	0.149	0.151	0.168 ± 0.003
(4, 2, 0)	0.123	0.118	0.121	0.132 ± 0.003
(4, 2, 2)	0.095	0.092	0.096	0.108 ± 0.004
(3, 3, 3)	0.086	0.085	0.089	0.109 ± 0.003
(5, 1, 1)	0.042	0.039	0.045	0.036 ± 0.004
(4, 4, 0)	0.045	0.045	0.049	0.058 ± 0.004
(5, 3, 1)	0.027	0.026	0.032	0.032 ± 0.004
(4, 4, 2)	0.038	0.038	0.042	0.052 ± 0.004
(6, 0, 0)	−0.013	−0.014	−0.005	−0.025 ± 0.003
(6, 2, 0)	−0.008	−0.009	−0.001	−0.009 ± 0.004
(5, 3, 3)	0.019	0.019	0.024	0.036 ± 0.004
(6, 2, 2)	−0.005	−0.005	0.001	0.006 ± 0.004
(4, 4, 4)	0.018	0.019	0.023	0.037 ± 0.004
(5, 5, 1)	0.002	0.003	0.008	0.009 ± 0.004
(7, 1, 1)	−0.033	−0.034	−0.025	−0.047 ± 0.004
(6, 4, 0)	−0.006	−0.006	0.000	−0.001 ± 0.004
(6, 4, 2)	−0.004	−0.003	0.002	0.001 ± 0.004
(5, 5, 3)	0.003	0.004	0.008	0.012 ± 0.004
(7, 3, 1)	−0.022	−0.022	−0.015	−0.027 ± 0.004
(8, 0, 0)	−0.045	−0.045	−0.036	−0.063 ± 0.004
(7, 3, 3)	−0.015	−0.014	−0.008	−0.017 ± 0.004

improved methods of $\vec{k}$-space integration.

Charge and spin densities at a nuclear site have been obtained, and are given in Table III. The effective hyperfine fields due to spin polarization, −69.7 kG for KSG and −57.6 kG for vBH potentials, are in rather good agreement with the experimental value of -76 ± 1 kG.[13] Our results include the modification of the core wave functions in the crystal environment but neglect all relativistic corrections (including a possible orbital field resulting from spin-orbit coupling). The use of Gaussian orbitals makes it more difficult to obtain accurate value for $|\psi(0)|^2$ than if Slater orbitals are employed. On the basis of comparison of free-atom wave functions we estimate the uncertainty in $|\psi(0)|^2$ due to use of Gaussian rather than Slater orbitals is less than 4% for all states. The difference between majority and minority spin densities should not be significantly affected by this. The spin densities along three principal directions are compared in Fig. 2. An overall reduction of the difference in spin densities due to electron correlation is found. Corresponding results for the normalized spin density form factor are given in Table IV. These are computed with (a) $g = 2$ and (b) no allowance for an orbital contribution. The core-electron contribution is included. Both the departure of g from 2 and the orbital moment are results of spin-orbit coupling and are neglected here. Our results are compared with the previous calculation of Wakoh and Yamashita,[14] and the experimental results of Mook.[15] The form factor from the KSG potential agrees better with the experimental values than that from the vBH potential for small K. All calculated points tend to fall consistently below experiment for larger K. Also, the anisotropy, which can be studied by comparing values of the form factor for two different vectors with equal values of $|\vec{K}|$, is too small.

We have also calculated the charge density form factor $\rho(\vec{K})$. These quantities can be measured in x-ray diffraction experiments. Our results are given in Table V where they are compared with other theoretical values and with experiment. There are evidently substantial disagreements between the results of different experimental groups.

The density of states has been calculated using the linear analytic tetrahedron method.[10] The combined density of states for both spins according to the KSG and vBH potential is shown in Figs. 3 and 4, respectively. Numerical values of the density of states at the Fermi energy are 22.92/(atom Ry) (KSG) 25.45/(atom Ry) (vBH). Both are much smaller than the value obtained from the electron specific heat,[19] 2.97/(atom eV) which is equivalent to 40.41/(atom Ry). This discrepancy probably indicates the presence of a large renormalization effect due to the electron-phonon interaction. The main majority spin peak in the density of states is 0.7 eV below the Fermi energy for the KSG potential and 0.5 eV below for the vBH potential.

In addition, we have investigated Fermi-surface cross sections in some symmetry planes. Since our calculations do not include spin-orbit coupling, we do not see here the hybridization of majority and minority spin sheets, and the consequent avoided crossings.[2] However, except near crossings our Fermi surface should be reliable. Spin-orbit coupling is a small effect except where degeneracies are removed. Our cross sections in (100) and (110)

TABLE V. Charge-density form factor.

Wave vector $a\vec{K}/2\pi$	Present KSG	Present vBH	Wakoh and Yamashita (Ref. 14)	Diana, Mazzone, and DeMarco (Ref. 16)	Hoyoswa and Fukumachi (Ref. 17)	Arii *et al.* (Ref. 18)
(0, 0, 0)	28.00	28.00	28.00			
(1, 1, 1)	20.39	20.43	20.28	20.10 ± 0.16	20.78	
(2, 0, 0)	19.05	19.08	19.05	18.55 ± 0.16	19.29	19.17 ± 0.17
(2, 2, 0)	15.39	15.40	15.35	15.34 ± 0.12	15.60	
(3, 1, 1)	13.57	13.58	13.47		13.63	
(2, 2, 2)	13.06	13.07	12.96		13.09	
(4, 0, 0)	11.47	11.47	11.35	11.18 ± 0.11	11.49	
(3, 3, 1)	10.52	10.52	10.47		10.61	
(4, 2, 0)	10.28	10.28	10.21		10.31	
(4, 2, 2)	9.40	9.40				
(3, 3, 3)	8.88	8.88		8.74 ± 0.09		
(5, 1, 1)	8.92	8.93		8.73 ± 0.09		
(4, 4, 0)	8.23	8.24				
(5, 3, 1)	7.93	7.93				
(6, 0, 0)	7.87	7.87				
(4, 4, 2)	7.82	7.82				

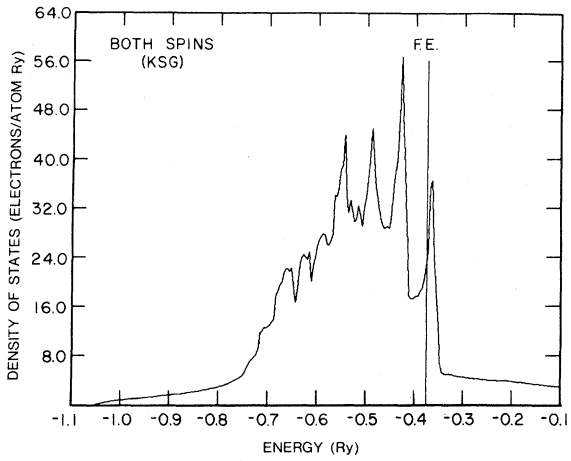

FIG. 3. Combined density of states (both spins) according to KSG exchange potential.

planes are shown in Figs. 5 and 6. Dotted lines represent results from the KSG potential; dashed lines, the vBH potential. The unpublished experimental results of Stark[2] for the large portions of the Fermi surface and the results of Tsui[20] concerning the hole pocket at X are also included for comparison. There is very little difference between the curves from different potentials in regard to the minority spin X_5 hole pocket (a) and the Γ center sp square (e). The vBH potential agrees with experiments better than KSG potential for the majority spin Γ centered sp square (d) and the neck around L_2' but the situation is reversed in the large minority spin Γ centered d sheet in the (110) plane. Both potential predict an extra $X_{2\downarrow}$ hole pocket which has not been observed experimentally. The partial inclusion of electron correlations in the vBH potential lead to a reduction of the separation between $X_{2\downarrow}$ and Fermi energy by about 0.002 Ry and hence slightly reduced the area of the unobserved hole pocket.

The persistence of this piece of Fermi surface may indicate the inadequacy of neglecting the density gradient term in the density functional formalism. We speculate that an inhomogeneity correction involving second-order terms in $\nabla\rho$ might push $X_{5\downarrow}$ (t_{2g} symmetry) and $X_{2\downarrow}$ (e_g symmetry) apart so that the latter would be below the Fermi energy, and thus eliminate the unobserved $X_{2\downarrow}$ hole pocket. The opposite displacement of X_5 would enlarge the light hole pocket which would also improve agreement with experiment.

The discrepancy observed in the anisotropy of the magnetic form factor; that the theoretical anisotropy is too small, can be interpreted in a related manner. Weiss and Freeman have shown that the Fourier transform of the charge density of spin-σ $3d$ electrons in a cubic field can be approxi-

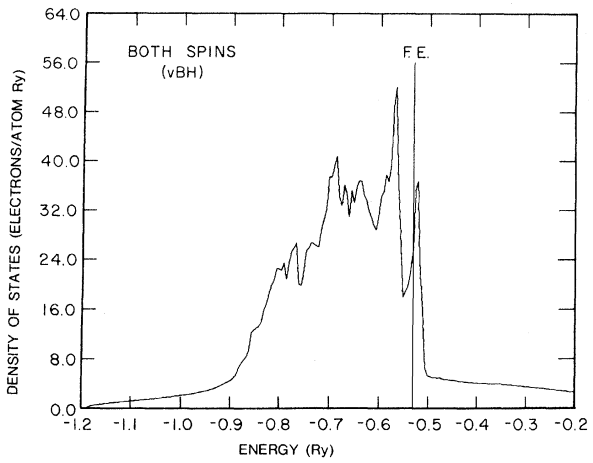

FIG. 4. Combined density of states according to the vBH potential.

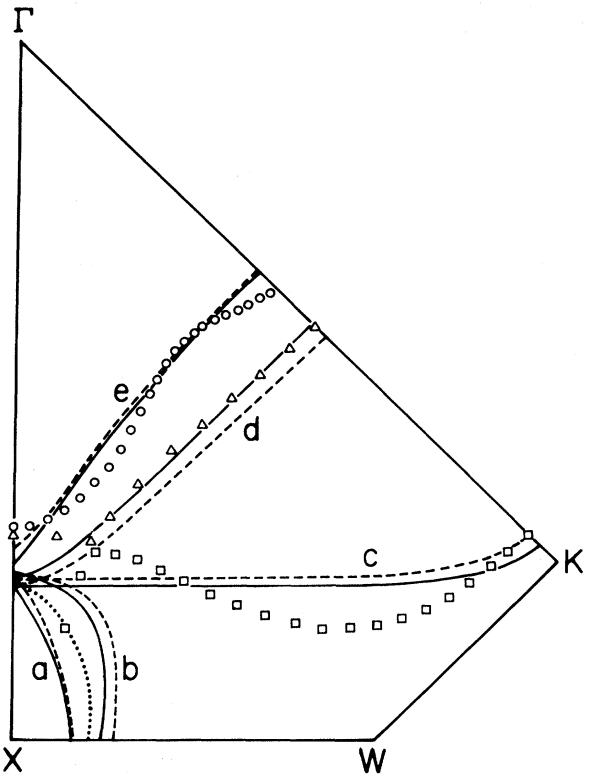

FIG. 5. Cross sections of the Fermi surface in the (100) plane. The dashed lines represent the results from the KSG potential, the solid lines those of the vBH potential. The circles, triangles, and squares are the experimental results of Stark; the dotted line, the experimental results of Tsui. The surfaces are designated by letters: a is the $X_{5\downarrow}$ hole pocket; b, the $X_{2\downarrow}$ hole pocket; c, the major $d\downarrow$ hole surface; d, the $sp\uparrow$ surface; e, the $sp\downarrow$ surface.

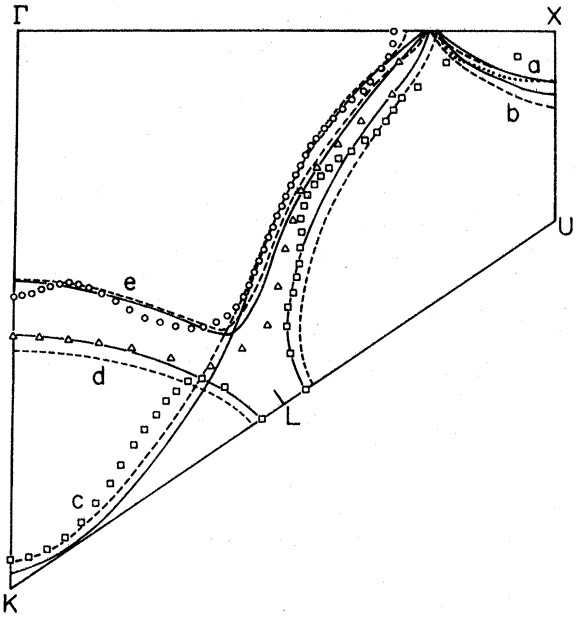

FIG. 6. Cross sections of the Fermi surface in the (110) plane. The notation is the same as in Fig. 5.

mated as[21]

$$f_\sigma(\vec{K}) = \langle j_0 \rangle_\sigma + (\tfrac{5}{2}\gamma_\sigma - 1) A(\vec{K}) \langle j_4 \rangle, \tag{7}$$

where $\langle j_0 \rangle_\sigma$ involves the spherical part of the distribution and $\langle j_4 \rangle_\sigma$ the aspherical part. The averages are taken over the distribution of electrons of spin σ. The quantity γ_σ is the fraction of $3d$ electrons of spin σ which have e_g symmetry. The angular dependence is described by

$$A(\vec{K}) = \frac{K_x^4 + K_y^4 + K_z^4 - 3(K_x^2 K_y^2 + K_y^2 K_z^2 + K_z^2 K_x^2)}{(K_x^2 + K_y^2 + K_z^2)^2} . \tag{8}$$

Let us consider the difference between the form factors for

$$\vec{K} = [333] \quad \text{and} \quad \vec{K} = [511]$$

as an example. If we neglect the spin dependence of $\langle j_4 \rangle$, it is straightforward to show that for the net spin-density form factor,

$$f_N(333) - f_N(511) = -1.317(\tfrac{5}{2}\gamma_N)\langle j_4 \rangle . \tag{9}$$

The quantity γ_N in (9) should be interpreted as $\gamma_\uparrow - \gamma_\downarrow$; the difference between the fraction of e_g character in the majority and minority spin density. We argue that $\gamma_\uparrow \sim 0.4$ since the majority spin d band is occupied, and $\gamma_\downarrow > 0.4$ since most of the $d_\downarrow$ holes are t_{2g}. $\gamma_\downarrow$ would be further increased if the minority spin $X_2(e_g)$ level were pushed below the Fermi energy by an inhomogenity correction. The net effect would then be an increase in the directional anisotropy of the spin form factor.

IV. CONCLUSIONS

We have compared the results of two band calculations for nickel that are identical except for the choice of exchange (or exchange-correlation) potential. The standard KSG potential ($X\alpha$ with $\alpha = \frac{2}{3}$) yields a rather good Fermi surface, except that there is an "extra" hole pocket ($X_{2\downarrow}$). The magneton number is, however, significantly too large, and the exchange splitting of the d-band states also appears to be considerably too large, although there is no accurately known experimental value. Wave-function properties (hyperfine field, charge, and spin form factors) appear to be fairly good. They are, however, subject to still uncalculated corrections for spin-orbit coupling and other relativistic effects. There are interesting indications that the failure of the calculations to produce enough anisotropy in the spin form factor may be correlated with the errors in the band structure, and possibly imply that inhomogeneity corrections to the potentials may be important.

The vBH potential leads to a significant improvement in the magnetic moment and the exchange splitting. The magnetic moment is quite close to the experimental value, but the calculated spin splitting may still be too large. Further experimental work on this question is urgently required. Elsewhere, we have suggested that precise measurements of optical properties in the 0.5-eV region would be particularly desirable.[2] The Fermi surface resulting from the vBH potential shows relatively minor differences from the KSG potential. There is probably an overall improvement, although it is not clear just what is the precision of the incompletely published experimental measurements. Values of wave-function properties move away from experimental results slightly; however, no particular conclusions can be drawn from this since relativistic effects are not included.

*Supported in part by the U. S. National Science Foundation.

[1]J. Callaway and C. S. Wang, Phys. Rev. B 7, 1096 (1973).
[2]C. S. Wang and J. Callaway, Phys. Rev. B 9, 4897 (1974).
[3]W. Kohn and L. J. Sham, Phys. Rev. 140, A1133 (1965); R. Gaspar, Acta. Phys. Acad. Sci. Hung. 3, 263 (1954).
[4]U. von Barth and L. Hedin, J. Phys. C 5, 1629 (1972).
[5]A. J. H. Wachters, J. Chem. Phys. 52, 1033 (1970).

[6]J. Callaway and J. L. Fry, in *Computational Methods in Band Theory*, edited by P. M. Marcus, J. F. Janak, and A. R. Williams (Plenum, New York, 1971), p. 512.
[7]C. S. Wang, Ph.D. thesis (Louisiana State University, 1974) (unpublished).
[8]R. C. Chaney, T. K. Tung, C. C. Lin, and E. E. Lafon, J. Chem. Phys. 52, 361 (1970).
[9]R. C. Chaney and F. Dorman, Int. J. Quantum Chem. 8, 465 (1974).
[10]G. Lehmann and M. Taut, Phys. Status Solidi 54, 469 (1972).
[11]J. Rath and A. J. Freeman, Phys. Rev. B 11, 2109 (1975).
[12]H. Dannan, R. Heer, and A. J. P. Meyer, J. Appl. Phys. 39, 669 (1968).
[13]J. C. Love, F. E. Obenshain, and G. Cizek, Phys. Rev. B 3, 2827 (1971).
[14]S. Wakoh and J. Yamashita, J. Phys. Soc. Jpn. 30, 422 (1971).
[15]H. A. Mook, Phys. Rev. 148, 495 (1966).
[16]M. Diana, G. Mazzone, and J. J. DeMarco, Phys. Rev. 187, 973 (1969).
[17]S. Hoyosawa and T. Fukumachi (unpublished) quoted by S. Wakoh and T. Yamashita, Ref. 14.
[18]T. Arii, R. Uyeda, O. Terasaki, and D. Watanabe, Acta. Crystallogr. A 29, 295 (1973).
[19]M. Dixon, F. E. Hoare, T. M. Holden, and D. E. Moody, Proc. R. Soc. A 285, 561 (1965).
[20]D. C. Tsui, Phys. Rev. 164, 669 (1967).
[21]R. J. Weiss and A. J. Freeman, J. Phys. Chem. Solids 10, 147 (1959).